THE UNIVERSITY of EDINBURGH

Edinburgh Research Explorer

Effect of flange and stiffener rigidity on the boundary conditions and shear buckling stress of plate girders

Citation for published version:
Al-Azzawi, Z, Stratford, T, Rotter, J & Bisby, L 2015, Effect of flange and stiffener rigidity on the boundary conditions and shear buckling stress of plate girders. in 15th European Bridge Conference & Exhibition. ECS Publications, Edinburgh.

Link:
Link to publication record in Edinburgh Research Explorer

Document Version:
Publisher's PDF, also known as Version of record

Published In:
15th European Bridge Conference & Exhibition

OPEN ∂ ACCESS

EFFECT OF FLANGE AND STIFFENER RIGIDITY ON THE BOUNDARY CONDITIONS AND SHEAR BUCKLING STRESS OF PLATE GIRDERS

Zaid Al-Azzawi*, Tim Stratford, Michael Rotter, Luke Bisby
The University of Edinburgh
School of Engineering,.
The King's Buildings
Edinburgh, EH9 3JL, UK.
z.al-azzawi@ed.ac.uk

KEYWORDS: Bridges, Steel structures, Plate girders, Shear buckling stress, Flange rigidity, Stiffener rigidity, initial imperfection.

ABSTRACT

The two essential functions of the web plate in a plate girder are to maintain a relative distance between the top and bottom flanges and to resist shear stresses. In most practical ranges of plate girder bridge spans, the shear stresses are relatively low compared to bending stresses in the flanges induced by flexure. As a result, the web plate is typically much thinner than the flanges. The web panel is therefore prone to buckling at comparatively low shear forces. To enhance the web's buckling strength, it is often reinforced with transverse stiffeners. The web design then involves a selection of plate thickness and stiffener spacing to provide optimum economy in terms of the material and fabrication costs.

In the design of plate girder web panels, according to AISC, AASHTO and EN 1993-1-5 specifications, the post-buckling strength is added to the elastic buckling strength. To calculate the elastic buckling strength, the boundary conditions of the web panel that is stiffened by transverse intermediate stiffeners must be determined.

In current practice, the elastic shear buckling stress of a web panel with transverse stiffeners is estimated using the conservative assumption that the web panel has simply supported boundary conditions at the junctions with the flange and the stiffener. The study presented herein explores this assumption using a more realistic approach, both numerically, through approximately 5000 numerical analysis runs, and experimentally. The results indicate that more realistic boundary conditions and critical buckling shear stress estimation could be obtained by accounting for the rigidity of the flanges and the stiffeners, in addition to initial web imperfections.

INTRODUCTION

Web buckling in shear is essentially a local buckling phenomenon, often with stable post-buckling behaviour. Depending upon the geometry, the web plate may carry loads considerably in excess of the initial buckling value at which the web starts to buckle; this is due to post-buckling strength. Taking advantage of this reserve strength, a plate girder of high strength/weight ratio can be achieved. Despite early work on web shear post-buckling behaviour (Wilson, 1886), and diagonal tension field theory developed later by Wagner (1931), elastic buckling was used as the basis for design of plate girder webs until the 1960s. This was largely because formulas to predict the elastic bifurcation buckling strength of a web plate are relatively simple, and have been known for many years, whereas a comprehensive and simple procedure for ultimate strength design was not available.

In the late 1950s, extensive studies were undertaken on the post-buckling behaviour of web panels by Basler and Thurlimann (1959). As a result of these and subsequent studies (Basler, 1961a, 1961b and 1963), AISC added the post-buckling strength into its specifications in 1963, and AASHTO followed suit in 1973. Thereafter, with the move towards limit state design concepts in steel structures, the studies initiated by Basler and Thurlimann were followed by several modified failure theories to achieve a better correlation between theory and tests (Lee et al., 1996).

In both the AISC and AASHTO specifications, the post-buckling strength is added to the elastic buckling strength. To calculate the elastic buckling strength, the boundary conditions of the web panel that is stiffened by transverse intermediate stiffeners must be determined. It is generally assumed that transverse

stiffeners are sufficiently stiff to form nodal lines of the sinusoidal buckling waves on the web. This assumption is well justified, since the transverse stiffeners are designed to meet this condition. On the other hand, the web panel is elastically restrained at the junction between the web and flanges. The degree of the elastic restraint depends on many geometric parameters, such as a_w/h_w, h_w/t_w, b_f/h_w, t_f/t_w, and t_s/t_w, where a_w is the transverse stiffener spacing, h_w is the girder depth, b_f is the flange width, t_f is the flange thickness, t_s is the stiffener thickness, and t_w is the web thickness. Although the notion of the real boundary condition at the juncture of the web and flanges to be somewhere between simple and fixed has been recognized for some time, it has always been idealised, mainly due to lack of means to evaluate it in a rational manner. For example, Basler (Basler, 1963) and Porter et al. (Porter et al., 1975) assumed that the web panel was simply supported at the junction, while Chern and Ostapenko (Chern and Ostapenko, 1969) obtained the ultimate strength by assuming that the junction was a fixed support. AISC and AASHTO specifications follow Basler's procedure, in which the boundary condition at the is conservatively assumed to be pinned.

Another controversial aspect of this problem is that the Cardiff method (Porter et al., 1975) places a much greater demand on stiffener strength than does Hoglund's rotated stress field theory (Hoglund, 1973). The Cardiff method requires the stiffeners to play the role of compression members in a truss, with the web plate acting as a tension diagonal. Hoglund's theory requires the stiffeners only to carry the small part of the tension field anchored by the flanges at collapse; no force is induced in the stiffeners in mobilising the post-critical resistance of the web. In the absence of a stiff flange to contribute to the shear resistance, the stiffeners only elevate the elastic critical shear stress of the web. Adequate stiffness is simply required to ensure that the theoretical elastic critical shear resistance of the panel is achieved, or at least very nearly achieved since no stiffener can be completely rigid.

Earlier drafts of EN 1993-1-5 required web stiffeners to be designed for a force loosely (but not exactly) based on Hoglund's theory, together with a check for adequate stiffness. These early drafts raised concern in the UK because the rules indicated that much smaller forces are induced in the stiffeners than would be derived from the tension field theory approach traditionally used in BS 5400: Part 3. As a result, late in its drafting EN 1993-1-5 was modified to include a stiffener force criterion more closely aligned to that in BS 5400: Part 3. The rules for stiffener design in EN 1993-1-5 are thus no longer consistent with the rotated stress field theory and indicate that a significantly greater axial force acts in the stiffener, with a consequent loss of economy. However, the rules for design of the web panel remain based on Hoglund's rotated stress field theory, creating an inconsistency (Hendy and Presta, 2008).

This inconsistency lead back to the subject of this study: what boundary conditions are realistic for both the stiffener and flange junctures with the web, because underestimating them will lead to uneconomic and conservative design while on the other hand overestimating the boundary conditions could reduce safety, especially when fatigue is taken into considerations. Therefore, an extensive parametric study of approximately 5000 specimens were tested numerically using finite element analysis, to find the effect of flange and stiffener rigidities in addition to the effect of initial imperfection on the critical buckling shear stress of plate girders.

ELASTIC BUCKLING STRENGTH IN PURE SHEAR STRESS
The elastic buckling strength in Basler's approach as well as in the Cardiff method is calculated considering the web panel simply supported on all sides. According to Timoshenko (1961):

$$\tau_{cr} = \frac{k_s \pi^2 E}{12(1-v^2)} \left(\frac{t_w}{h_w}\right)^2 \tag{1}$$

where
  τ_{cr} : elastic buckling shear stress of web panel
  t_w : web plate thickness
  h_w : web plate height
  E : Young's modulus
  v : Poisson's ratio
  k_s : shear buckling coefficient

$$k_s = 5.34 + \frac{4.0}{(a_w/h_w)^2} \qquad a_w/h_w \geq 1 \qquad\qquad\qquad (2.a)$$

$$k_s = 4.0 + \frac{5.34}{(a_w/h_w)^2} \qquad a_w/h_w < 1 \qquad\qquad\qquad (2.b)$$

where

a_w : is the space between vertical stiffeners

Fujii, on the other hand, recommends fixed condition for the web sides along the flanges. The shear buckling coefficient for this condition is given in graphical form by fujii and as regression formula derived by Bulson (1970) as illustrated in the work done by Lee et al. (1996):

$$k_{sf} = 8.98 + \frac{5.61}{(a_w/h_w)^2} - \frac{1.99}{(a_w/h_w)^3} \qquad\qquad a_w/h_w \geq 1 \qquad\qquad (3.a)$$

$$k_{sf} = \frac{5.34}{(a_w/h_w)^2} - \frac{2.31}{(a_w/h_w)} + 8.39(a_w/h_w) - 3.44 \qquad a_w/h_w < 1 \qquad (3.b)$$

Based on over 300 numerical results, Lee et al. (1996) proposed the following two simple equations:

$$k = k_s + \frac{4}{5}\left(k_{sf} - k_s\right)\left[1 - \frac{2}{3}\left(2 - \frac{t_f}{t_w}\right)\right] \qquad \frac{1}{2} < \frac{t_f}{t_w} < 2 \qquad\qquad (4.a)$$

$$k = k_s + \frac{4}{5}\left(k_{sf} - k_s\right) \qquad\qquad\qquad \frac{t_f}{t_w} > 2 \qquad\qquad\qquad (4.b)$$

where k_s and k_{sf} are as mentioned above.

EXPERIMENTAL WORK AND RESULTS

In order to start the project with certain limits for the geometrical boundary conditions of the web plate boundaries, we needed to verify whether there is a possibility to reach the fixed boundary conditions experimentally.

To achieve this goal, a new testing rig (Picture Frame) is introduced. This Picture Frame is capable of holding the steel plate, applying fixed boundary conditions and in-plane shear loading simulating a real plate girder shear test, see Fig. (1-a). The Picture Frame is built on the idea of clamping the steel plate boundaries into a very stiff steel frame using bolts that does not infiltrate the steel plate itself in order to avoid stress concentrations within the plate. This Frame is capable of moving only in-plane using a 4-hinge beam chain mechanism and thus applying shear force upon the steel plate relying only on the friction between the Picture Frame and the steel plate. This in-plane movement is achieved by using 8 hinges instead of 4 to avoid cutting the steel plate corners which will affect the stress distribution and to make sure that the loads are applied throughout the plate corners for better simulation of buckling of steel plates under shear loading.

The validity of the design for this Picture Frame was established through finite element simulations, which included modelling different scenarios of the Picture Frames with respect to the boundary conditions applied on the steel plate, the location of the hinges and the distribution of the stresses developed in each component of the frame and the tested steel plate. Fig. (1-b) shows a photo of the Picture Frame final setup.

The tested plate dimensions were 500x500x2mm with an aspect ratio of 1.0 and a slenderness ratio of 250. Fig. (2) shows the applied shear stress versus the central out-of-plane displacement for the tested specimen. The experimental value of the critical buckling shear stress was 42.5 MPa corresponding to 42.54 MPa in theory for fixed boundary condition. The plate had an initial imperfection of 0.4mm and it was tested using a 1000 kN Instron actuator with a stroke of 1.0 mm/min. The data were recorded using Microlink 3000 data acquisition system at a rate of 1.0 Hz.
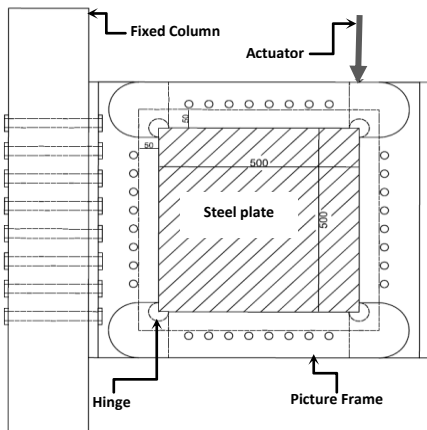
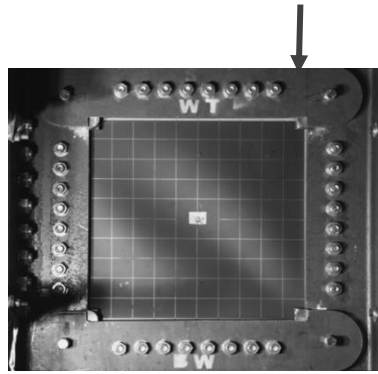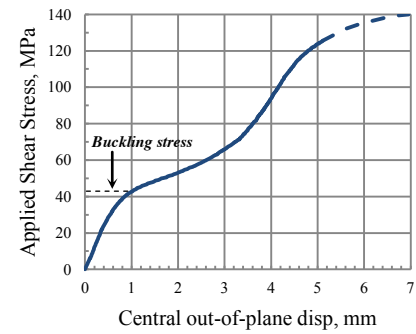Fig. (1-a): Picture frame diagram.

Fig. (1-b): Picture Frame.

Fig. (2): Buckling results.

FINITE ELEMENT ANALYSIS

Analytical Model

Fig. (3-a) shows the plate girder model adopted in this study. In studying the critical buckling shear stresses, the researchers usually model one panel from the plate girder, but in this study, two panels were modelled to take the stiffener effect on the buckling shear stress into account in addition to the usual flange effect. The stiffener effect is usually neglected in the calculations and simply supported boundary conditions in the junction between the web plate and the stiffener is assumed. In this study, single one sided whole height stiffener was used with three different projected widths (b_s) of 70, 110, 140mm. This was done to take the effect of rigidity of the stiffener and its second moment of area on the geometrical boundary conditions at the junction with the web plate. The figure also shows the load pattern which was necessary to simulate the case of pure shear so we can compare it with the theory. The width of the flange (b_f) was chosen to be 340 mm which satisfies most of the available standards for plate girder design, but with minimum requirements, this is to ensure that worst case scenario is taken into account in this study, and hence it is safely applicable for other range of flange widths. It is worth mentioning that all other model dimensions were taken similar to a previous study by Lee et al. (2002) for the sake of comparison. In their study, they were trying to find out the effect of stiffener on the postbuckling strength of plate girders, while in this study it is used to find the effect of stiffener on the critical buckling shear stress but with much wider range of variables. The yield strength (f_y), Poisson's ratio (v), and the modulus of elasticity (E) were taken as 355MPa, 0.3, and 200 GPa, respectively, and were kept constant in this study.

Finite Element Model

The finite element model used in this study is shown in Fig. (3-b). The height of the model (h_w) was kept constant at 2000mm while the span was variable to account for different aspect ratios (a_w/h_w). The model was built using S9R5 element type, which is not available in Abaqus standard CAE and can be used only through Abaqus input file. Matlab code was written to create the parts' nodes and element incidences and then the input file was created. The element S9R5 deals mostly with slender plates and was derived originally according to Kirchhoff thin plate bending theory. The size of the web elements was chosen to be $h_w/20$ based on an extensive convergence study, while the size of the flange and stiffener elements were taken equal to 100×20mm and 50×20mm, respectively and it was validated through another convergence study. The applied boundary conditions are illustrated in Table (1).

Table (1). Boundary conditions used for the model

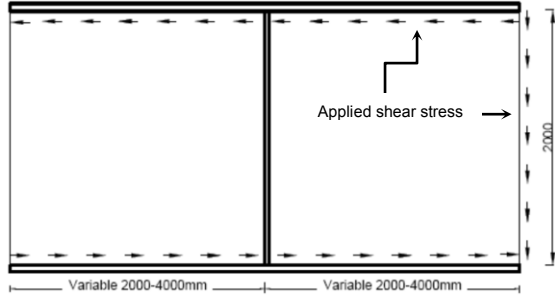|		u	v	w	θ_x	θ_y	θ_z
Flange	Left	Fix	Fix	Fix	Fix	Fix	Free
	right	Free	Free	Fix	Fix	Fix	Free
Web	Left	Fix	Fix	Fix	Fix	Free	Fix
	right	Free	Free	Fix	Fix	Free	Fix

Fig. (3-a): Plate girder analytical model.
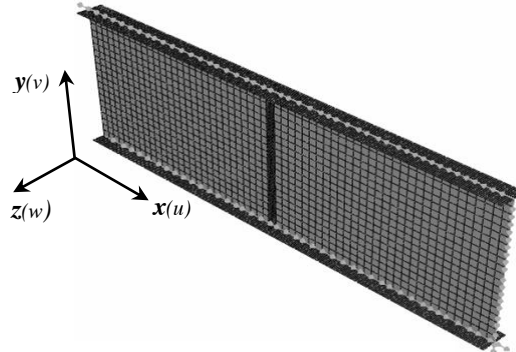
Fig. (3-a): Finite element model.

Convergence Study

The model adopted in the convergence study was chosen to be a typical web plate with practical dimensions of 2000×2000mm. The plate aspect ratio was taken as $a_w/h_w=1.0$ and kept constant throughout the convergence study. The variables were the type of the element (S4R, S8R, and S9R5) and the slenderness ratio (h_w/t_w) which were taken as 1000, 500, 250, 200, 166.667, 142.857 and 125 corresponding to a plate thicknesses of 2, 4, 8, 10, 12, 14, and 16, respectively. Both simply supported and clamped boundary conditions were investigated and shear stress was applied to the plate boundaries exactly like the main model in Fig (3-a).

Fig. (4) shows typical curves for the critical buckling shear stress versus the inverse of the degrees of freedom (dof) for a specimens with clamped boundary conditions and slenderness ratio of 125, 200, and 500, respectively. The dof was calculated each time according to the number of element used and the corresponding degrees of freedom of each node in the element according to the compatibility requirement. Using the inverse of dof gave us the opportunity to predict the element size that will give us exactly the same theoretical value or as close as possible. S9R5 showed superior behaviour with much less number of elements and the size of $h_w/20$ (100mm) was chosen. This size helped in reducing the time required for the huge number of simulation runs we had without compromising convergence.
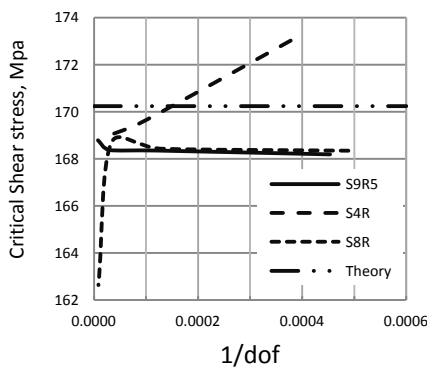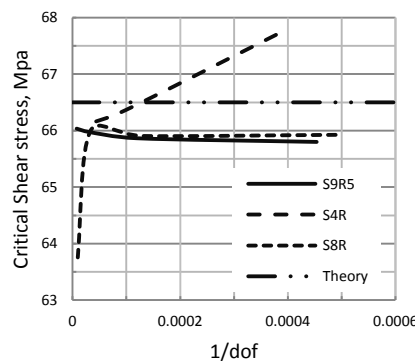

Fig. (4-a): $h_w/t_w = 125$
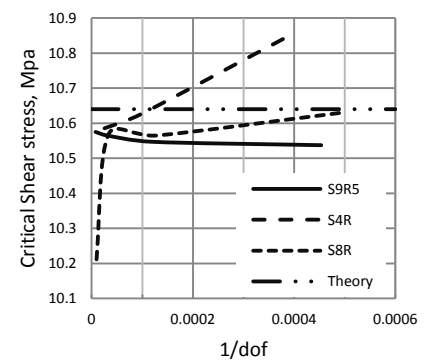

Fig. (4-b): $h_w/t_w = 200$

Fig. (4-c): $h_w/t_w = 500$

Fig. (4): Critical buckling shear stress versus the inverse of the degrees of freedom.

Parametric Study

An extensive parametric study with approximately 5000 numerical analysis has been performed. The key variables were the aspect ratio (a_w/h_w), the slenderness ratio (h_w/t_w), the stiffener projected width (b_s), the flange thickness (t_f), the stiffener thickness (t_s), and the effect of initial imperfection (*ii*). The range of variables was as follows:

a_w/h_w = 1.0- 2.0   with a_w = 2000- 4000 mm,
h_w/t_w = 125- 250   with t_w = 8- 16 mm,

b_s = 70- 150 mm,
t_f = 2- 50 mm,
t_s = 2- 50 mm,
ii   = $h_w/125000$- $h_w/100$; with a_w/h_w = 1.0.

In order to present the flange rigidity effect on the critical buckling shear stress, a dimensionless parameter which was originally proposed by Rockey and Skaloud in 1972 is used. The same approach was applied to predict the stiffener rigidity effect in this study as follows:

$$R_F = \frac{I_F}{a_w^3 \, t_w} \tag{5.a}$$

$$R_S = \frac{I_S}{h_w^3 \, t_w} \tag{5.b}$$

Where:
  R_F: is the flange rigidity index.
  R_S: is the stiffener rigidity index.
  I_F : is the flange second moment of area of an axis passing through the centroid of the flange and normal to the web plate.
  I_S : is the second moment of area of the projection of the T-section formed from combining the stiffener and the web plate.

Fig's. (5-a)- (5-f) show the relation between critical buckling shear stresses coefficient and the flange & stiffener rigidity indexes. There is a dominant pattern where the effect of the flange starts increasing sharply at lower flange thicknesses, and then reaches a plateau where increasing the flange thickness does not increase the buckling coefficient any more. This behaviour is more revealed with higher slenderness ratios. The same behaviour does not apply for the stiffener effect where increasing its second moment of area has an average linear pattern. However, this increase in the buckling coefficient due to stiffener rigidity is reduced with increasing the aspect ratio of the specimens to be insignificant and almost flat with an aspect ratio of 2.

Fig's. (6-a)- (6-c) demonstrate the buckling modes for three models with heavy (t_f=50mm), medium (t_f=26mm), and light (t_f=2mm) flange having the same aspect ratio (a_w/h_w=1.5), slenderness ratio (h_w/t_w=167), and stiffener dimensions (110×26mm), these are the middle range of the variables in this study. It is obvious that the behaviour gets stiffer with increasing the flange thickness.
On the other hand Fig's (6-d)- (6-f) show the buckling modes for three models with heavy (t_s=50mm), medium (t_s=26mm), and light (t_s=2mm) stiffener having the same abovementioned parameters, except that the flange is kept constant with a thickness of (t_f=26mm). Again we can see that the behaviour is getting stiffer with increasing the stiffener thickness and hence the assumption that the boundary condition in the junction between the stiffener and the web plate is merely simply supported is not valid all the time and more investigation is needed.
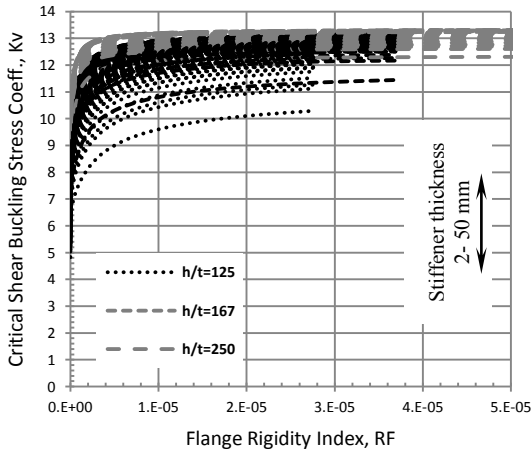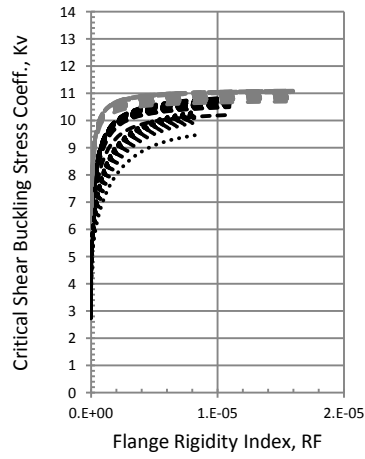
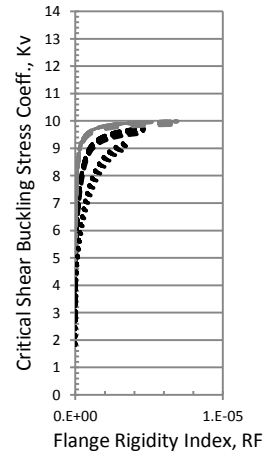Fig. (5-a): $a_w/h_w = 1.0$

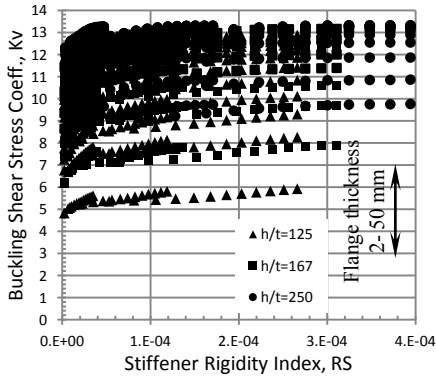Fig. (5-b): $a_w/h_w = 1.5$

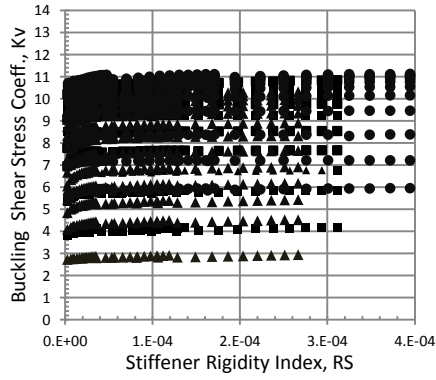Fig. (5-c): $a_w/h_w = 2.0$

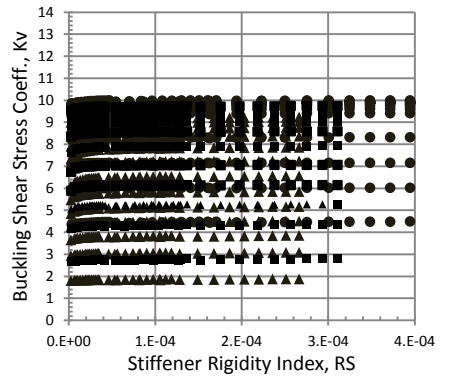Fig. (5-e): $a_w/h_w = 1.0$

Fig. (5-e): $a_w/h_w = 1.5$

Fig. (5-f): $a_w/h_w = 2.0$

Fig. (5): Critical buckling shear stress coefficient versus flange and stiffener rigidity indexes.
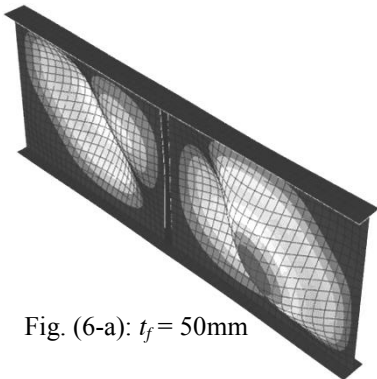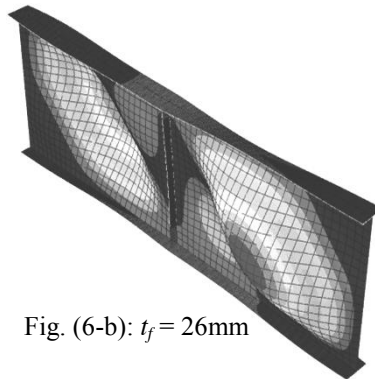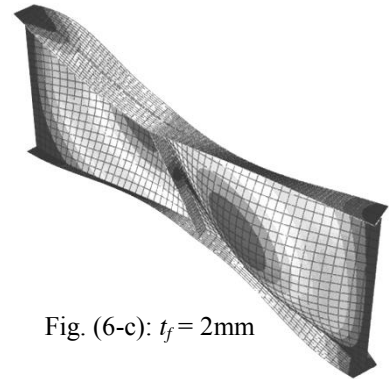

Fig. (6-a): $t_f = 50$mm

Fig. (6-b): $t_f = 26$mm

Fig. (6-c): $t_f = 2$mm
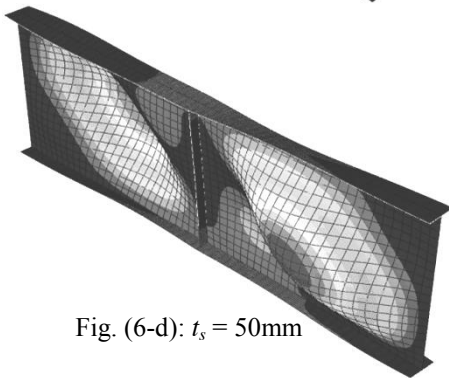
Fig. (6-d): $t_s = 50$mm

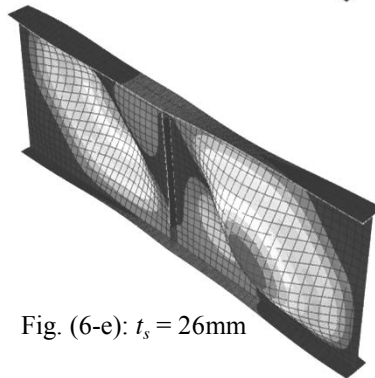Fig. (6-e): $t_s = 26$mm
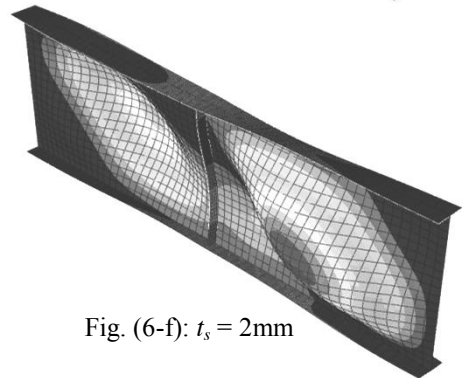
Fig. (6-f): $t_s = 2$mm

Fig. (6): Buckling modes of the plate girder model for different parameters.

ANALYSIS OF RESULTS AND DESIGN APPROACH

Fig's (7-a) to (7-c) show how the calculated critical buckling shear stress coefficient varies with the non-dimensional parameter (t_f/t_w) for an aspect ratio (a_w/h_w) of 1.0, 1.5, and 2.0, respectively. Only data with practical design ranges of t_f/t_w and $t_s/t_w \geq 1.0$ were considered in the analysis. The figures corresponding to an aspect ratio of 1.5 and 2.0 show the same pattern where the curves forms bundles of data according to their slenderness ratio and thus can be treated as on curve. This means that the effect of stiffener on the critical buckling shear stress coefficient is insignificant and can be neglected just like all the standards does. However this behaviour does not apply for the specimens with an aspect ratio of 1.0. It is well demonstrated throughout Fig. (7-a) that the data are more scattered but in a homogeneous pattern leading to the fact that the stiffener effect is significant and it should be taken into account.

Another important conclusion can be drawn from these figures, which is that the buckling coefficient are rather higher than the simply supported boundary condition case and the effect of flange rigidity in the junction between the flange and the web panel should be taken into consideration which is in agreement with the conclusion of Lee et al. (1996).

Applying Lee et al. equation (Eq. 4) as shown in Fig's (7-a) to (7-c) show that some of the data points of this study are out of its bounds and it is not safe to use the equation for all the data ranges. However, the equation is simple, powerful, and can still be used with some modifications to account for the new findings in this study.

Modifying Eq. (4) to account for the new data in this study will result in the following new equation:

$$k = k_s + \frac{4}{5}\left(k_{sf} - k_s\right) \times \left[1 - \frac{1}{1.5}\left(3 - \frac{t_f}{t_w}\right)\right] \qquad 1.5 < \frac{t_f}{t_w} < 3 \qquad (5.a)$$

$$k = k_s + \frac{4}{5}\left(k_{sf} - k_s\right) \qquad\qquad\qquad \frac{t_f}{t_w} > 3 \qquad (5.b)$$

where k_s and k_{sf} are the same as in Eqs. (2) and (3).

In addition to this, the following modifications and restrains should be taken into consideration:

- The effect of stiffener rigidity on the critical buckling shear stress coefficient for specimens with an aspect ratio $a_w/h_w \leq 1.0$ may be taken as follows:

$$k_{stiffener\ Effect} = k + \left(0.5\ ln\left(\frac{t_s}{t_w}\right)\right) \qquad (5.c)$$

- k_s must be reduced for specimens with slenderness ratio $h_w/t_w \leq 125$ by the following factor:

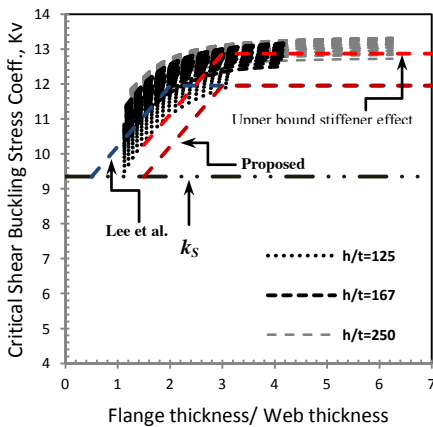$$k_{125\ Effect} = k - \left(\frac{a_w}{h_w} - 1\right) \qquad (5.d)$$
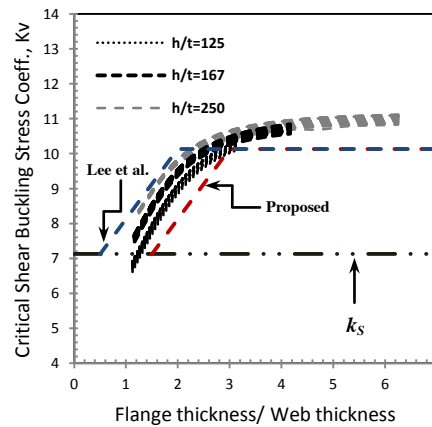

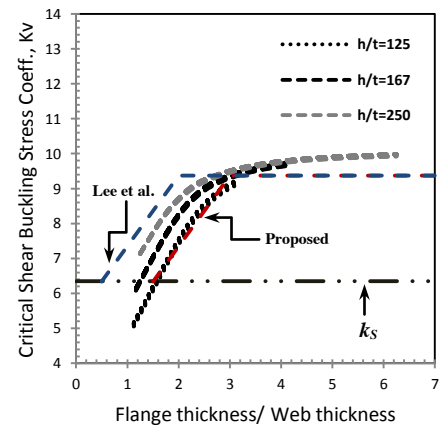Fig. (7-a): $a_w/h_w = 1.0$ Fig. (7-b): $a_w/h_w = 1.5$ Fig. (7-c): $a_w/h_w = 2.0$

Fig. (7): Design envelops for the critical buckling shear stress coefficient.

INITIAL IMPERFECTION EFFECT

Irrespective of the degree of sophistication of the numerical method used, the main drawback of any procedure attempting to use numerical results as a basis for deriving design data remains the uncertainty related to the magnitudes and distributions of the initial deformations and residual stresses (Grondin et al., 1999). Initial imperfections in structures that have not been subjected to damage loads usually result from the fabrication process.

According to all the international standards the authors are aware of, initial distortion (or variation from flatness) for web panels with intermediate transverse stiffener is allowed and the maximum varies from $d/80$ to $d/130$ depending upon panel dimensions and stiffener configurations, where d is the lesser dimension of the stiffener spacing (a_w) and the web height (h_w). Previous studies have shown that, as the initial out-of-flatness increases, the bending stresses are significantly magnified, resulting in reduced ultimate shear strength especially for web panels with low slenderness ratios (h_w/t_w) where the membrane action is not dominant (Lee et al., 1998).

However, in this study we are trying to predict the effect of initial imperfection on the critical buckling shear stress in both aspects of its magnitude in comparison to the theory and its behaviour demonstrated in the buckling curves.

Among several imperfection types, only web initial out-of-flatness is considered, the effect of stiffener imperfection is not considered in this study. Three types of initial out-of-flatness are considered, namely, initial imperfection similar to the expected buckling modes (+buckle), initial imperfection against the expected buckling modes (-buckle), and a neutral buckling mode which lies in the middle between the first two types (neutral). Fig's. (8-a) to (8-c) show prototypes of the three initial imperfection types considered in this study.

The first two types of the initial imperfection (+buckling and –buckling) were found using the elastic Eigen buckling modes. These modes were initiated using the buckling analysis available in Abaqus CAE and then imposed as an initial imperfection using Abaqus script commands in the input file. The third type of the initial imperfection (neutral) was created via Matlab where the web was created with the required initial imperfection using a double trigonometric series as follows:

$$u(x,y) = w_o \, sin\left(\frac{n\pi x}{a_w}\right) sin\left(\frac{m\pi y}{h_w}\right) \tag{6}$$

where w_o is the central initial imperfection and n & m were taken equal to 1.0 for simplicity.

After that, a full geometrical and material nonlinear analysis (MGNA) was performed to find the overall behaviour of the specimen up to failure. The same boundary conditions and material properties were used except that a constant strain hardening of (E/100) was added to the steel stress strain curve to account for material nonlinearity. The validity of the model was proven in a separate study by the authors which still under publication.
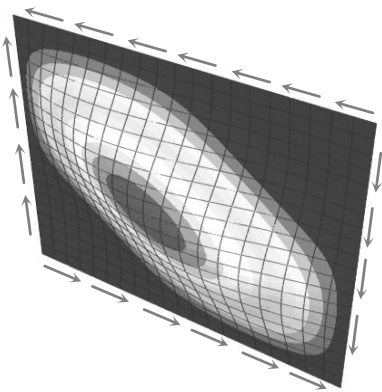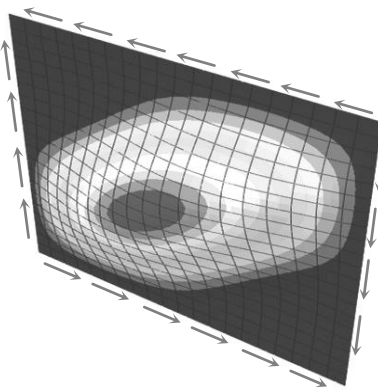

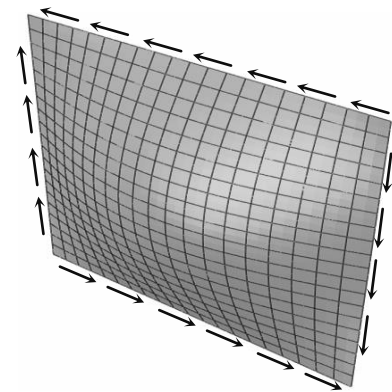Fig. (8-a): +buckling *ii* pattern   Fig. (8-b): -buckling *ii* pattern   Fig. (8-c): neutral *ii* pattern

Fig. (8): Illustration of the three initial imperfection types adopted in this study.

Fig's. (9-a) to (9-c) compare the applied shear stress versus the web central out-of-plane displacement (to be called buckling curves from now on) for specimens with initial imperfection $ii = h_w/1250$ and $ii = h_w/125$ for the three imperfection categories we introduced in this study, (+buckling, -buckling, and neutral). The figures show that the buckling stress is strongly dependent on both the magnitude and type of initial imperfection and this phenomena increase with decreasing the slenderness ratio from 250 to 125. This could be related to the dependency of the boundary condition at the junction of the web plate with the flange and stiffener on the relative thickness of the three of them (i.e. t_f/t_w and t_s/t_w). In addition to that, the figures show that the specimens with small initial imperfection ($h_w/1250$) tend to buckle almost at the same proposed buckling stress, while specimens with higher initial imperfection tend to buckle with a lower stress than the proposed one, meaning that a reduction factor must be included to account for initial imperfection for specimens with high initial imperfection.

This reduction factor can be expressed as follows:

$$\sigma_s^R = \sigma_{ss} + \left[\left(\frac{\sigma_s^p - \sigma_{ss}}{\frac{h_w}{125} - \frac{h_w}{1250}} \right) \left(\frac{h_w}{125} - \frac{h_w}{w} \right) \right] \tag{7-a}$$

$$w = \frac{h_w}{w_o} \tag{7-b}$$

where

σ_s^R : is the reduced buckling shear stress due to initial imperfection, MPa,

σ_s^P : is the buckling shear stress calculated according to the proposed buckling coefficients, MPa,

σ_{ss} : is the critical buckling shear stress with simply supported boundary conditions, MPa,

w_o : is the central out of flatness of the web plate, mm.

Eq. (7-a) can be approximated and further simplified with a maximum error of 2.2% as follows:

$$\sigma_s^R = \sigma_{ss} + \left[(\sigma_s^p - \sigma_{ss}) \left(1 - \frac{125}{w} \right) \right] \tag{7-c}$$

The effect of the type of initial imperfection is well obvious in Fig. (9) and it affects both the critical buckling stress as well as the ultimate shear capacity of the specimen. However, in this study we are more concerned with buckling stresses. As can be seen from Fig. (9), specimens with +buckle type initial imperfection have always the lowest buckling stress and specimens with –buckle type initial imperfection have always the highest buckling stress, while the specimens with neutral type of initial imperfection always lie between the two of them. This increase in the buckling stress of –buckle type specimens maybe related to the additional energy required to reform and alter the buckling mode from a –buckle mode to a +buckle mode. The –buckle imperfection mode acts as prestressing to the web plate and increases its buckling stress while the +buckle imperfection mode does not require the same amount of energy as it is already took the required shape for the buckling to initiate.
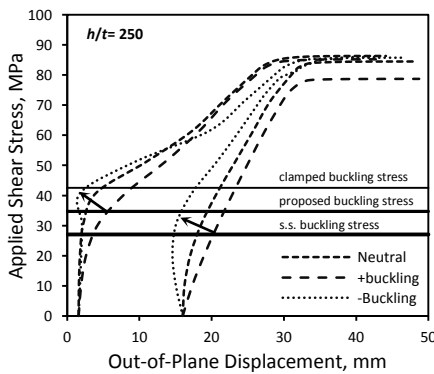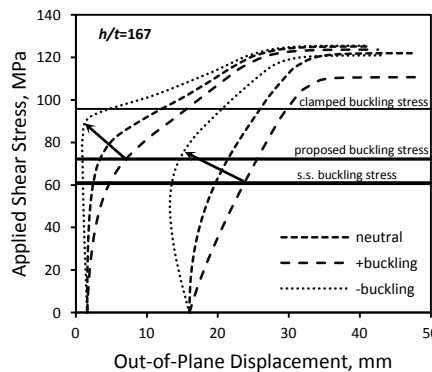

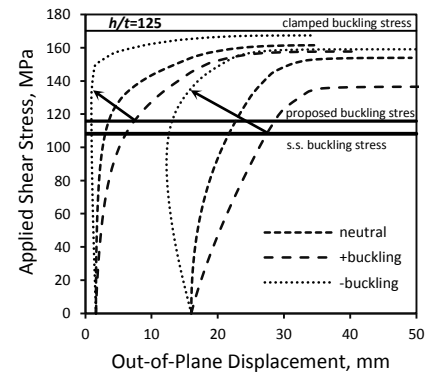Fig. (9-a): h_w/t_w =250   Fig. (9-b): h_w/t_w =167   Fig. (9-c): h_w/t_w =125

Fig. (9): Applied shear stress versus web central out-of-plane displacement for specimens with initial imperfection.

Another observation can be drawn from Fig. (9) is that there is a difficulty with locating the buckling stress for neutral and –buckle imperfection specimens. This can be overcome by drawing a normal line from the +buckle imperfection mode curve at the point of the buckling stress to the other curves and their interchange can be considered as the buckling stress. This phenomena is observed in the 81 curves we have in this study for the initial imperfection effect and may be called the Normality method.

CONCLUSIONS

In spite of the fact that critical bucking shear stress of plate girders loaded mainly in shear have been studied for so many years by multiple researchers, but the matter of choosing the right boundary conditions at the junction between the web plate and the flange & stiffener is still a problem of Engineering judgment and standards approach. To the knowledge of the authors, all current codes of practice and standards adopt a conservative design criterion by taking the simply supported boundary conditions at this junction. However, in this study, we have proved experimentally that the fixed boundary conditions at the web junctions could be reached. This was accomplished by using a specially designed testing rig (Picture Frame), which is capable of holding the web plate with fixed boundary conditions at its boundaries and applying in-plane shear stress.

This conclusion led us to an extensive parametric study with approximately 5000 numerical test using finite element method to investigate the effect of the flange and stiffener rigidity on the boundary conditions at the web plate boundaries in steel plate girders.

The results of this study came in agreement with previous studies which stated that the simply supported boundary conditions are conservative and could lead to uneconomical design especially for thin-walled plate girders (i.e. specimens with high slenderness ratio). Some of these previous researches proposed a mixed simply supported and fixed boundary conditions for the web plate junction with the stiffener and flange, respectively. They proposed new equations to account for this buckling stress increase, such as the work by Fujii which was adopted later by Lee et al.

In this study, a modified equation for determining the critical buckling shear stress coefficients is proposed. The original equation was proposed by Lee et. al (1996), but some of the numerically tested specimens in this work was found out of its bounds leading to a non-safe design. This equation was modified using the data analysed in this study and a new modified equation is presented.

The effect of stiffener rigidity is neglected by all previous studies which assumed conservatively that the stiffener is stiff only enough to provide simply supported boundary condition at its junction with the web plate. In this study, we found that this is true for specimens with aspect ratio, $a_w/h_w > 1.0$, while this is not true for specimens with aspect ratio, $a_w/h_w = 1.0$. An equation taking the stiffener rigidity effect in increasing the buckling coefficient is proposed.

Finally, the effect of initial imperfection is studied for different magnitudes and different imperfection categories, namely; +buckle, -buckle, and neutral. A full GMNA was performed using Abaqus and the results showed a typical pattern were the buckling stress was reduced with increasing the initial imperfection and a novel equation taking this reduction into account is proposed.

REFERENCES

- AASHTO, Standard Specifications for Highway Bridges, 11th Edn. American Association of State Highway Officials, Washington, DC (1973).
- AISC, Specification for the design, Fabrication and Erection of Structural Steel for Building, 6th Edn. American Institute of Steel Construction, New York (1963).
- British Standards Institution, Code of Practice for Design of Steel Bridges, Milton Keynes, BSI 1982, BS 5400: Part 3.
- Bulson P. S., Stability of Flat Plates, Elsevier, (1970) New York.

- C. Chern and A. Ostapenko, Ultimate strength of plate girder under shear. Fritz Engineering Laboratory. Report No. 328.7, Lehigh University (1969).
- C. R. Hendy and F. Presta, Transverse web stiffeners and shear moment interaction for steel plate girder bridges, The Structural Engineer, Nov. 2008, pp. 13-26.
- CEN, Eurcode 3: Design of Steel Structures, Part 1.5: Plated structural elements, Milton Keynes, BSI, 2004, ENV 1993-1-5.
- D. M. Porter, K. C. Rocky and H. R. Evans, The collapse behaviour of plate girders loaded in shear. Struct. Engnr 53, 313-325 (1975).
- G.Y. Grondin, A.E. Elwi, and J.J.R. Cheng, Buckling of stiffened steel plates- a parametric study, Journal of Constructional Steel Research 50 (1999), pp. 151-175.
- H. Wagner, Flat sheet metal girder with very thin metal web. National Advisory Committee for aeronautics (NACA), Tech, Memo. Nos. 604, 605, 606 (1931).
- Hoglund T., Design of thin plate I girders in shear and bending with special reference to web buckling, Bulletin No. 94 Division of Building Statics and Structural Engineering, Royal Institute of Technology, Stockholm, Sweden, 1973.
- J. M. Wilson, On Specifications for strength of iron bridges. Trans. ASCE, 15, 401-403 and 489-490 (1886).
- K. Basler and B. Thurlimann, Plate girder research. In: Proc. AISC National Engineering Conf. New York (1959).
- K. Basler, New provisions for plate girder design. In: Proc. AISC National Engineering Conf. New York pp. 65-74 (1961a).
- K. Basler, Strength of plate girders in shear. Trans. ASCE 128,683-719 (1963).
- K. Basler, Strength of Plate girders under combined bending and shear. J. Struc. Div. ASCE 87, 181-197 (1961b).
- K. C. Rockey and M. Skaloud, The ultimate load behaviour of plate girders loaded in shear. The Structural Engineer, No. 1, Vol. 50, Jan. 1972, pp.29-47.
- S. C. Lee, J. S. Davidson and C. H. Yoo, Shear buckling coefficients of plate girder web panels, Computers & Structures, Vol. 59, No 5, pp. 789-795, 1996.
- S.C. Lee and C.H. Yoo, Strength of Plate Girder Web Panels Under Pure Shear, J. Struct, Eng. 1998.124, pp. 184-194.
- S.C. Lee, H. Yoo, and Y. Yoon, Behavior of intermediate transverse stiffeners attached on web panels, Journal of Structural Engineering, March 2002, pp.337-345.
- Timoshenko, S. P. and Gere, J. M., Theory of Elastic Stability, 2nd Edition, McGraw-Hill (1961) pp 151-180.